Electrospun fibers of poly (vinyl alcohol): zinc acetate (PVA:AcZn) and further ZnO production: evaluation of PVA:AcZn ratio and annealing temperature effects on ZnO structure

Vitor H. B. Oliveira · Elisangela P. da Silva · Vicente de S. Marques · Adley F. Rubira · Rafael Silva · Carlos E. Cava · Sidney A. Lourenço · Edvani C. Muniz ⬡

Abstract The effects of the poly (vinyl alcohol): zinc acetate (PVA:AcZn) mass ratio on the morphology and structure of the precursor electrospun fibers as well as the calcination conditions on the morphology and chemical and physical structure of the as-obtained zinc oxide (ZnO) nanofibers are deeply discussed in this work. Initially, precursor nanofibers were obtained through electrospinning, a simple and accessible process for the production of materials in nano- and sub-micrometric scales, of aqueous solution of poly (vinyl alcohol) (PVA) and zinc acetate (AcZn) in the mass ratios PVA:AcZn 1:0.5, 1:1, and 1:2. In the sequence, the precursor nanofibers were calcined (500, 600, and 700 °C, for 2 h in atmospheric air) to obtain the ZnO fibers. The precursor PVA:AcZn and the ZnO fibers were characterized through Fourier transform infrared spectroscopy (FTIR), thermogravimetry (TG), X-ray diffractometry (XRD), X-ray scattering spectroscopy (EDS), Raman spectroscopy, and scanning electron microscopy (SEM). The set of results indicates that the ZnO fibers with the best characteristics (homogeneity in morphology, smaller average diameter, organization of the crystalline structure, among others) were obtained using mass ratio of PVA:AcZn 1:1 and calcination at 600 °C for 2 h in atmospheric air.

Keywords Electrospinning · Nanofibers · Poly (vinyl alcohol) · Zinc acetate · ZnO nanofibers

V. H. B. Oliveira · C. E. Cava · S. A. Lourenço · E. C. Muniz
Post-graduation Program in Material Science and Engineering, Federal University of Technology–Paraná, Londrina, PR 86036-370, Brazil

E. P. da Silva (✉) · A. F. Rubira · R. Silva · E. C. Muniz
Department of Chemistry, State University of Maringa, Avenida Colombo 5790, Maringá, PR 87020-900, Brazil
e-mail: elisangelapachecodasilva@gmail.com

V. de S. Marques · E. C. Muniz (✉)
Department of Chemistry, Federal University of Piauí, Campus Universitário Ministro Petrônio Portella, Teresina, PI 64049-550, Brazil
e-mail: ecmuniz@uem.br

e-mail: edvanimuniz@utfpr.edu.br

e-mail: munizec@ufpi.edu.br

Introduction

One-dimensional (1D) structure materials, such as nano-rods, nanotubes, nanowires, and nanofibers, have been the focus of several kinds of research due to their large specific surface area, and special chemical and physical properties originating mainly from their size. These properties make 1D nanostructure intriguing for numerous applications (Zhao et al. 2019). A large number of fabrication methods have been demonstrated to produce different 1D nanostructure, including electrospinning hydrothermal, self-assembly, and isolation from natural sources, for instance (Cavaliere 2016). Among these methods, electrospinning is, from the technological

point of view, a very interesting strategy because the fibers can be obtained in nano- and sub-micrometric scales, with controlled orientation and morphologies. From an economic and industrial points of view, the electrospinning technique is also interesting because the equipment, on a laboratory scale, is very accessible and scalable, as compared to other processes (Merritt et al. 2012), for monitoring large quantities of nanofibers (Thenmozhi et al. 2017; Xue et al. 2019; Persano et al. 2013).

Electrospinning is a technique widely used for the production of fibers of diameters in the nano- and sub-micrometric scales, allowing high surface/volume ratio (Wang et al. 2020; Zhang et al. 2020; Ghafari et al. 2019). The principle of the technique consists in ejecting a polymeric solution that travels across an electric field created by connecting an external voltage source to a metallic (grounded) collector and to the capillary tube (normally, a metallic needle connected to a syringe from which the solution is ejected). In the trajectory capillary collector, the solvent evaporates and the polymeric material is deposited in the collector as fibers (Greiner and Wendorff 2007).

Zinc oxide nanofibers (ZnO) have attracted increased attention since it is an important semiconductor with unique properties and employed in different fields, such as catalysis (Wang et al. 2019), sensors (Kim et al. 2019), and optical devices (Kim et al. 2019; Li and Xia 2004). The interest for electrospun ZnO nanofibers has increased since the pioneer work by Yang et al. in 2004 (Yang et al. 2004; Sawicka and Gouma 2006). A very interesting application of ZnO nanofibers is as a basic material for gas sensors. For example, Shingange et al. (2019) developed an H_2S sensor based on ZnO nanofibers obtained through electrospinning and doped with La_2O_3. The authors found that the sensor has high selectivity, sensitivity, and reproducibility, as well as stability and rapid response for the detection of H_2S. Recent work developed in our research group shows that ZnO nanofibers chemically modified with L-cysteine can be used as high sensitivity sensor for detecting Pb^{2+} ions and can be noticed as another example of this type of application (Oliveira et al. 2020). In that work, the ZnO fibers were produced from calcination of PVA:AcZn electrospun nanofibers at 1:1 ratio obtained from the electrospinning of an aqueous PVA solution containing zinc acetate (PVA/AcZn). Other PVA:AcZn ratios did not show the same response as the ZnO fibers made through calcination at 600 °C of PVA:AcZn at 1:1

ratio. The detection limit of the Pb^{2+} sensor was 0.397 μg/L, showing high sensitivity and selectivity as compared to other sensors that are not based on ZnO nanofibers.

However, for production of metal oxide nanofibers through electrospinning, generally, a polymeric material is used as template to eject the solution and to polymeric/metal fiber formation (Zhang et al. 2019; Kantürk Figen and Coşkuner Filiz 2019). PVA is one of the most used polymers to produce nanofibers (Costa et al. 2019; Chamakh et al. 2020; Saveh-Shemshaki et al. 2019). PVA is a synthetic polymer that is hydrophilic, odorless, non-toxic, biocompatible (Alexandre et al. 2014), biodegradable (O'Donnell et al. 2020), with good flexibility and transparency (Peng et al. 2017), water resistant (Peng et al. 2017), with good ability to form films and good mechanical properties (Peng et al. 2017; Tian et al. 2018), and has high swelling properties (Xie et al. 2012), characteristics that expand the use of this polymer in several fields (Peng et al. 2017; Tian et al. 2018).

Accordingly, in this work, we present and discuss the effects of the PVA:AcZn mass ratio in the precursor solution on the morphology and average diameter of the PVA:AcZn nanofibers, as well as the effect of the calcination temperature on several properties of the ZnO fibers. The ZnO nanofibers were characterized through several techniques, such as SEM/EDS, FTIR, TG, Raman, and XRD.

Experimental

Materials

Poly (vinyl alcohol) (PVA) (Mw = 104.5 kDa) and degree of hydrolysis 87–89% was purchased from Neon (Suzano-SP, Brazil). Zinc acetate (AcZn), purity ≥ 98%, was purchased from Labsynth (Diadema-SP, Brazil). Zinc oxide (ZnO, powder), 99%, was purchased from Nuclear (Brazil). All reagents were used without prior purification.

Methods

Preparation of PVA-AcZn solutions

Aqueous solution of PVA 12.4% m/v (12.4 g in 100 mL of distilled water) was prepared under heating between

80 and 90 °C and magnetic stirring for 2 h for complete solubilization of the polymer and homogenization of the solution. Subsequently, aqueous solutions of AcZn were prepared at 10.0, 20.0, and 40.0%—m/v (from the solubilization of 300.0, 600.0, and 1200.0 mg of the solute in 3 mL of distilled water). Then, the AcZn solutions were poured into 5 mL of PVA solution to achieve the mass ratios PVA:AcZn (1:0.5, 1:1, and 1:2). The mixtures were stirred for about 3 min on a magnetic stirrer. Using the same procedure, a PVA solution (without AcZn) was also prepared and used for comparison. The solutions were identified by the mass ratio PVA:AcZn: 1:0, 1:0,5, 1:1, and 1:2.

Synthesis of PVA/AcZn and ZnO nanofibers

Aliquot of 5 mL of the PVA:AcZn solution was transferred into the syringe and then inserted into the injection pump of a homemade electrospinning apparatus. The distance of the needle ($\varnothing_{internal} = 0.7$ mm, 30-mm length) to the stainless steel collector (circular, static, $\varnothing = 15$ cm) was 15 cm. The applied voltage was 22 kV; and the solution was ejected from the syringe at a rate of 0.20 mL h^{-1}. The electrospun PVA/ZnAc fibers deposited in the collector were stored in a desiccator for 24 h followed by calcination in a furnace at 500, 600, or 700 °C for 2 h in atmospheric air. The following symbology was used to characterize the ZnO fibers: PVA:ZnO: 1:0.5 (500 °C), 1:0.5 (600 °C), 1:0.5 (700 °C), 1:1 (500 °C), 1:1 (600 °C), 1:1 (700 °C), 1:2 (500 °C), 1:2 (600 °C), and 1:2 (700 °C). For precursor fibers, the following notations were used: 1:0, 1:0.5, 1:1, and 1:2.

Characterization

Measurements of electrical conductivity of polymeric solutions were performed using the conductivity meter (MS Tecnopon Instrumentação, Brazil). FTIR spectra were obtained in a spectrometer (Perkin Elmer, EUA), model Spectrum Two, in a range of 400 to 4000 cm^{-1}. The morphology of materials was examined through a scanning electron microscope (FEI, USA), model Quanta 250, accoupled to EDS probe. The analyses of Zn, C, and O atom distribution in fibers before and after the annealing process were performed using energy-dispersive X-ray spectroscopy (EDS) coupled to a same SEM microscope. The mapping EDS was obtained using AZtec® software, applying a voltage of 20 kV and magnifications of × 15,000.

The average size diameter of ZnO nanofibers was obtained using Size Metter© software by counting around 40 fibers ($n = 40$) directly from SEM images. Thermogravimetric analyzes (TGA) were carried out in a TA thermo-analyzer (Shimadzu, Japan), model Q50, operating at following conditions: air stream of 50 mL min^{-1}, heating rate of 10 °C min^{-1}, and temperature range of 30–700 °C. Raman spectra were collected on a spectrometer (WITec, Germany), model Alpha 300, in a range of 200–700 cm^{-1} and using 532 nm as excitation wavelength. The crystalline structures were determined through wide-angle X-ray diffractometry (WAXD) using the LAB-X equipment (Shimadzu, Japan), model XRD D6000, equipped with a Co-Kα radiation source (40 kV and 30 mA). The diffractograms were recorded in a 2θ range of 10–80° with a scanning speed of 2.0 (deg min^{-1}). To calculate the size of the crystallites, the Debyer-Scherrer equation was used (Mustapha et al. 2019). The DC electrical conductivity was measured by the four-probe method using two digital multimeters (Minipa Mdm-8145). The powder of fiber samples was gently compressed inside a threaded tube (inner diameter 5 mm) with two stain steel screws at each tube ends. In the experiment, it is considered that the sample possesses ohmic behavior within the applied potential range (0–4 V):

$$\frac{1}{\rho} = \frac{h}{R \cdot A} \tag{1}$$

where R is the electrical resistance, A the internal area of the threaded tube, and h is the height of the sample layer in the tube that is determined by the distance between the face of the two screws in the tube.

Results and discussion

Several factors influence the properties of micro- and/or nanofibers obtained by the electrospinning technique, which can be categorized as follows (i) polymer properties, (ii) solution properties, (iii) process parameters, and (iv) environmental conditions (La Porta and Carlton 2020). In this work, the parameters related to the electrospinning process, such as concentration of the polymer, voltage of the applied electric field, distance from the needle-to-collector, and solution flow, as well

as the temperature, were kept constant in all the experiments carried out. The relative humidity of the air varied from 45 to 55%. The effects of adding different amounts of AcZn to the PVA solutions from which the precursor nanofibers were evaluated. Thus, the PVA solution was electrospun to obtain PVA nanofibers (1:0) and to serve as a basis for comparison to analyze the effect of salt on the precursor nanofibers. In addition, the conditions used for calcination can influence the properties of ZnO nanofibers. The expectation was that in the calcination process, there would be complete removal of the polymer and the formation of ZnO fibers, preferably highly crystalline. Thus, the PVA polymer was used as a template in the perspective that the ZnO nanofibers had the same morphology as the precursor fibers.

Morphological characterization and average diameter of nanofibers

The nanofibers obtained from the solution of PVA and PVA:AcZn at different mass ratios were characterized by SEM and EDS. SEM images and distribution histograms for the fiber diameters are shown in Fig. 1.

It is noted that the presence of AcZn induced some changes in the morphology of NFs compared to neat PVA NFs; despite that, they maintained to be smooth and randomly entangled. The presence of salt affects the diameter of the fibers. A decrease in the average diameter of the fibers obtained from the solutions containing AcZn was observed: the value changed from 455 nm in the fibers obtained from the PVA solution to 407 nm in the composite fibers 1:0.5. With a greater amount of AcZn in the solution to be electrospun, an even greater reduction in the average diameter of the fibers was observed, reaching 309 nm in the fibers at mass ratio PVA:AcZn 1:2. This reduction in the diameter of the fibers may be related to the presence of salt that increases the charge density of the solution as exposed to the electrical field during the electrospinning process. ZnO electrospun fibers can be also obtained through electrospinning of polymeric (polyvinylidene fluoride, PVDF) solution containing ZnO and further annealing. Han et al. showed in their study that the ZnO can help the precursor solution carry more electric charges, leading to the more electrostatic force on the ejecting solution (Han et al. 2019). In the presence of the electric field, the ionic species accommodate greater amount of electrical charges and induce higher stretching in the jet

ejected from the capillary. The repulsion among the excess charged moieties in the polymer chains exposed to the electric field results in finer and elongated fibers, and with narrower diameter distribution (Son et al. 2004). So, in the case of electrospinning of PVA solution containing AcZn, the more intense stretching induced to obtainment of thinner fibers as compared to electrospun PVA fibers.

As expected, the addition of AcZn affects the electrical conductivity of the solution, as compared to the PVA solution, as shown in Fig. 2. The presence of AcZn in the solution in the mass ratio 1:0.5 increases the conductivity of the solution by about ten times when compared to the PVA solution (1:0). Subsequent increases for AcZn lead to further increases in conductivity, however on smaller jumps. Thus, the reduction in the average diameter of the composite fibers is justified by the presence of salt in the solution submitted to electrospinning, which is in accordance with the literature data (Son et al. 2004).

Characterizations of the chemical groups present in the fibers

EDS analyses were performed to confirm the presence of AcZn in the precursor nanofibers and to evaluate the presence of possible contaminants. The EDS spectra of fibers 1:0, 1:0.5, 1:1, and 1:2 (Fig. 1(a$_2$–d$_2$)) show peaks attributed to the elements carbon, oxygen, and zinc, confirming the presence of AcZn and PVA in the precursor fibers.

PVA (1:0) and composite nanofibers (1:0.5, 1:1, and 1:2) were analyzed through FTIR. It was possible to identify the chemical groups present in the PVA nanofibers and in 1:0, 1:0.5, 1:1, and 1:2 fibers, as shown in the FTIR spectra of Fig. 3. The FTIR spectrum of 1:0 fibers showed characteristic bands, attributed to the polymer, at 3337 cm^{-1}, ascribed to the stretching O–H, 2934 cm^{-1}, assigned to the C-H from alkyls groups, 1724 cm^{-1}, corresponding to C=O from carbonyl groups, respectively (Thomas et al. 2001). The FTIR spectra of the precursor 1:0, 1:0.5, 1:1, and 1:2 fibers showed peaks at 1567 cm^{-1} and 1418 cm^{-1} attributed, respectively, to the symmetric and asymmetric stretching of carboxylate groups (COO$^-$) from acetate ions. Other bands at 1063 cm^{-1} and between 500 and 700 cm^{-1}, which were due to the deformation and frequency modes of the CH$_3$ group (Zhang et al. 2008) and the stretching modes of the Zn-O bond,
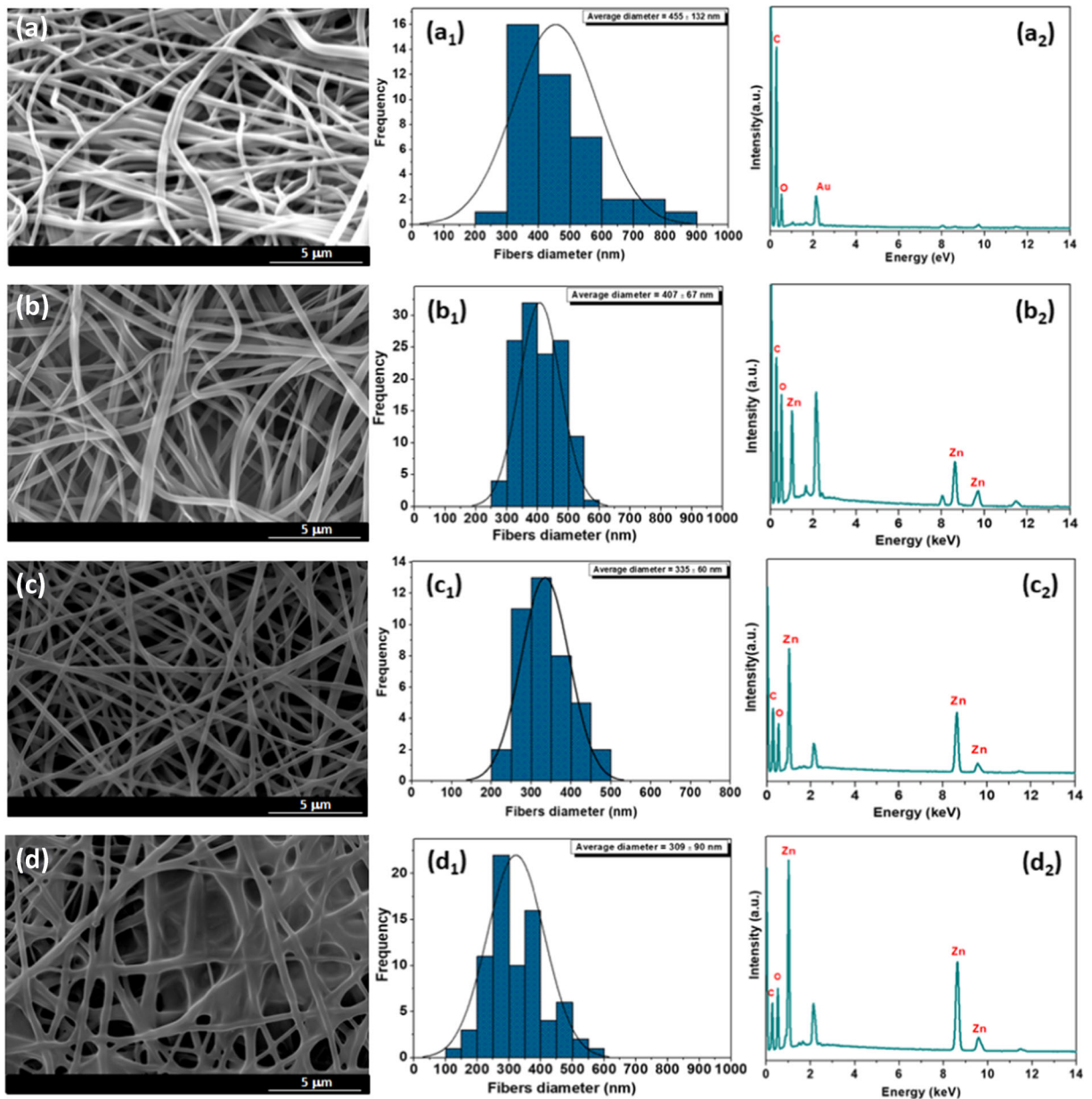
Fig. 1 SEM images of the fibers: (a) 1:0, (b) 1:0.5, (c) 1:1, and (d) 1:2; histogram of fibers diameter distribution: (a$_1$) 1:0, (b$_1$) 1:0.5, (c$_1$) 1:1, and (d$_1$) 1:2; EDS spectra of the fibers: (a$_2$) 1:0, (b$_2$) 1:0.5, (c$_2$) 1:1, and (d$_2$) 1:2

respectively, confirmed the formation of composite PVA/AcZn nanofibers. Table 1 summarizes the mentioned bands observed in the FTIR spectra PVA and PVA/AcZn fibers.

Analysis of thermal stability

Thermal stability of 1:0, 1:0.5, 1:1, and 1:2 nanofibers was investigated using thermogravimetry analysis and the TG curves are shown in Fig. 4. For 1:0 nanofibers, three stages of mass loss were observed. In the first stage, in the range of 30–80 °C, a loss of mass of 5% was observed, which is related to water evaporation. The other two stages of decomposition, between 80 and 480 °C, result from the decomposition of organic matter. In the range of 80–360 °C, a loss of mass of approximately 78% was observed. In this stage, the decomposition of organic matter probably occurred,
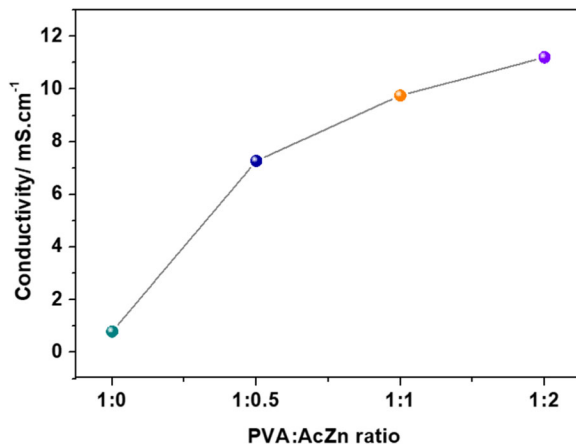
Fig. 2 Electric conductivity as a function of the PVA/AcZn mass ratio in the solutions submitted to electrospinning

which is mainly constituted by the amorphous part of the polymer. In the range of 360–480 °C, there is a loss of mass of 14%, which was related to the degradation of the highly stable crystalline parts of PVA (Budrugeac 2008). Above 480 °C, no loss of mass was observed, showing that up to this temperature all PVA is fully degraded and the waste is volatilized.

The composite nanofibers with the lowest amount of AcZn (1:0.5 ratio) presented 4 stages of decomposition: (a) region between 27 and 70 °C (5.5%), (b) region between 84 and 316 °C (39%), (c) region between 316 and 529 °C (14%), and (d) region between 529 and 793 °C (5%). The initial stages are due to the evaporation of the adsorbed water, the dehydration of crystalline water, and a slow partial decomposition of zinc acetate and PVA, while the final stages are due to the
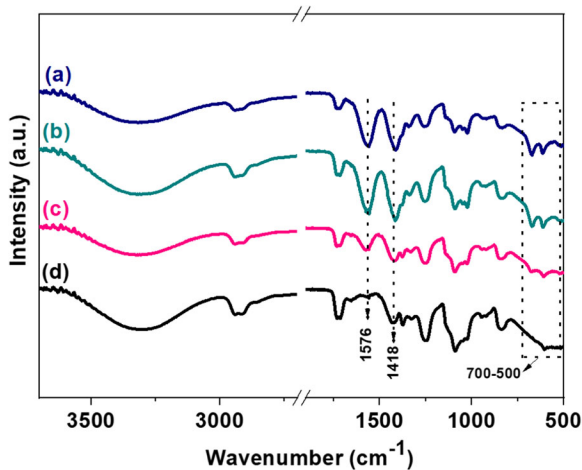
degradation of the organic matter of both PVA and zinc acetate, with a loss of mass of 19%. Six stages of mass loss were observed in 1:1 nanofibers, which are as follows: (a) in the region between 27 and 63 °C (10%), (b) between 64 and 148 °C (6%), (c) in the region between 149 and 210 °C (11%), (d) between 211 and 258 °C (21%), (e) region between 259 and 277 °C (8%), and (f) between 277 and 475 °C (24%). It can be said that stages (a) and (b) are due to the evaporation of adsorbed water, to the dehydration of crystalline water, and to the partial decomposition of AcZn and PVA, as observed for the 1:0.5 fibers. Stage (c) presented greater loss of mass; about 64% was degraded up to 475 °C. The last stages, (d) to (f), correspond to the degradation of organic matter from PVA and zinc acetate, indicating that this degradation occurs in different stages than the observed for the 1:0.5 fibers. Above 475 °C, the occurrence of mass loss was no longer observed, which indicates that the polymeric part (organic part of the composite fiber) was removed, resulting in 20% ZnO. This result is in accordance with observed by Ghafari et al. Such authors used DSC analysis to confirm that annealing temperature higher than 480 °C is required to remove the PVA, to decompose the zinc acetate, and to form crystalline ZnO nanostructure (Ghafari et al. 2017).

For 1:2 nanofibers, the same behavior was observed, that is, a degradation in six different stages, related to water evaporation and degradation of organic matter. However, a greater amount (27%) of ZnO was obtained, which was expected since a greater amount of AcZn was added to the 1:2 PVA:AcZn solution.

Characterizations of the ZnO fibers

After, thermal stability of the 1:0, 1:0.5, 1:1, and 1:2 fibers has been analyzed through TG curves; new samples of these fibers were calcined at temperatures of 500, 600, and 700 °C in order to obtain ZnO fibers and to evaluate the influence of annealing temperature on the properties of calcined fibers. Figures 5, 6, and 7 show the SEM images, the diameter distribution histograms, and the respective EDS spectra for nanofibers 1:0.5, 1:1, and 1:2 obtained by calcination at 500, 600, and 700 °C, respectively. It was observed that the annealing temperature has direct influence on the morphology and diameters of the as-obtained nanofibers but in a different way in relation to the initial PVA:AcZn mass ratio used in solution for obtaining the precursor fibers.

Fig. 3 FTIR spectra of nanofibers: 1:2 (a), 1:1 (b), 1:0.5 (c), and 1:0 (d)

Table 1 Attributions of the main FTIR bands of PVA nanofibers and composite PVA/AcZn nanofibers

Wavenumber (cm^{-1})	Characteristic groups	Assignment	Material
3337	O–H	Stretch	PVA
2934	C–H	Stretch	PVA
1724	C=O	Stretch	PVA
1576	O=C=O	Stretch	Zinc acetate
1418	=C–O$^-$	Asymmetric stretching	Zinc acetate
1063	–CH$_3$	Deformation	Zinc acetate
500–700	ZnO	Flexion type Vibration	Zinc acetate

The SEM image of 1:0.5 (500 °C) fibers (Fig. 5(a)) shows continuous and little roughness fibers, without the presence of nanograins. The largest amount of nanograins was observed in nanofibers 1:0.5 (600 °C) (Fig. 5(b)); however, the morphology of the fibers was maintained. The complete removal of the polymer occurred at 600 °C or above, and it is inferred that nucleation and growth of ZnO crystals may be associated with this behavior at that condition.

The SEM image of fibers 1:0.5 (700 °C) (Fig. 5(c)) indicates the formation of a large amount of interconnected grains. Analysis of the diameter of the fibers annealed at 700 °C shows reduction in the average diameter in relation to the respective precursor fibers, from 400 (before annealing) to 110 nm after. This drastic reduction in diameter is related to the removal of PVA that has fundamental role encapsulating the

precursor (AcZn) and, after annealing, to form the ZnO wires (Blachowicz and Ehrmann 2020). However, with the removal of the PVA fibers, beyond thinner, they become more fragile and are easily destroyed if handled without much care.

In relation to the SEM image of 1:1 (500 °C) fibers (Fig. 6(a)), the annealing at 500 °C was sufficient for the formation of ZnO grains, but some grains are not interconnected. As already discussed, there are still organic residues in the fibers. The SEM image of the 1:1 (600 °C) fibers (Fig. 6(b)) shows that the fibers are, in fact, made up of grains that come together to form continuous structures, like a pearl necklace, due to nucleation and the growth of ZnO crystallites. The diameter analysis showed that the 1:1 (600 °C) fibers obtained at this temperature possess an average diameter of 216 nm, also smaller than the average diameter of the

Fig. 4 TG curves of 1:0, 1:0.5, 1:1, and 1:2 electrospun fibers
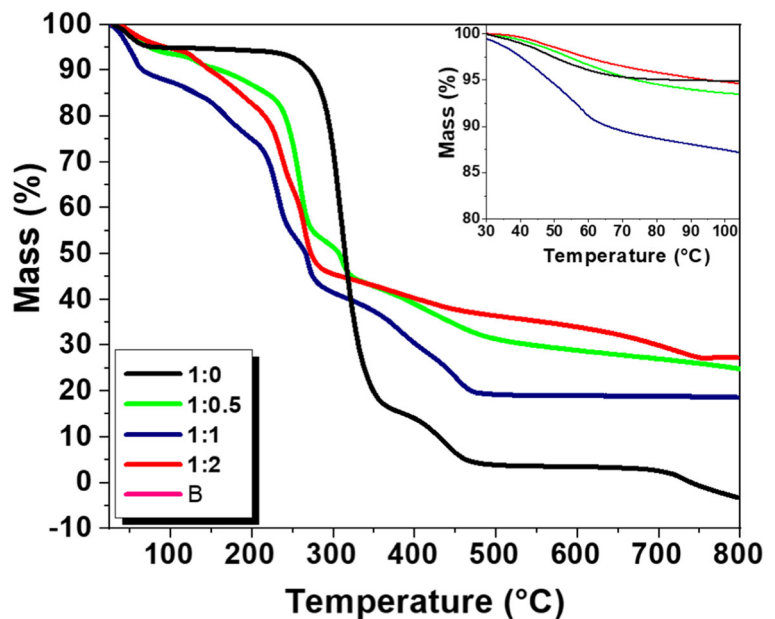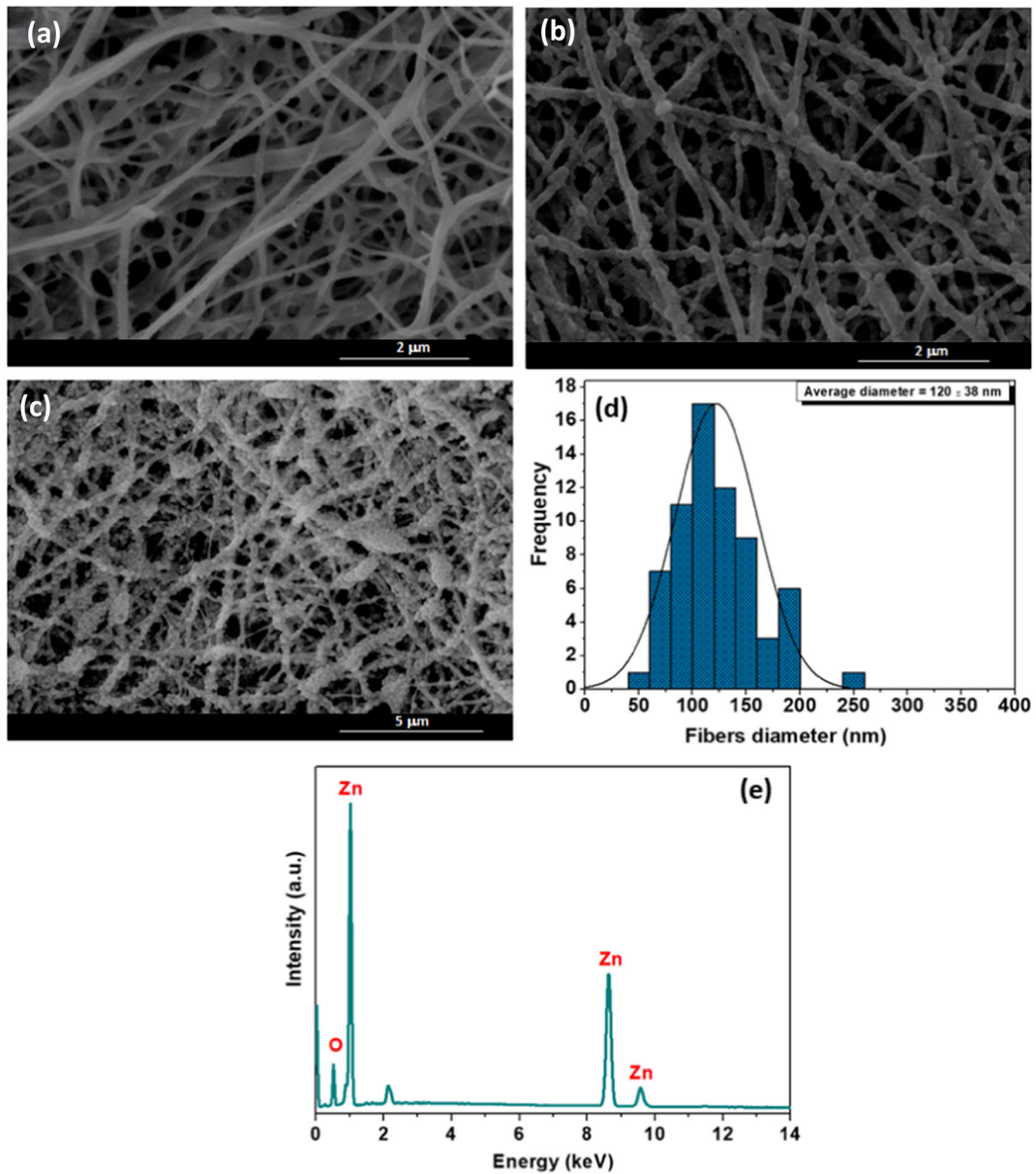
Fig. 5 SEM images of nanofibers: (a) 1:0.5 (500 °C), (b) 1:0.5 (600 °C), and (c) 1:0.5 (700 °C). (d) Diameter distribution histogram of 1:0.5 (500 °C) fibers. (e) EDS spectrum of 1:0.5 (500 °C)

precursor fibers (335 nm). In SEM image of 1:1 (700 °C) fibers (Fig. 6(c)), the average diameter decreased as compared to 1:1 (600 °C) ones and the material looks like a system with lesser interconnected particles.

The SEM images of the ZnO fibers obtained from a solution with a higher content of AcZn (mass ratio 1:2) are shown in Fig. 7. The fibers 1:2 (500 °C) (Fig. 7(a)) present a larger amount of agglomerated and connected

grains, but in fiber format. The increase in the annealing temperature favors the growth of the grains maintaining the fiber shape, as observed in the fibers calcined at 600 °C (Fig. 7(b)). If calcined at 700 °C (Fig. 7(c)), the grains maintain connectivity along the fibers. The average diameter of 1:2 (700 °C) nanofibers was 203 nm. So, at this temperature, the removal of the polymer strongly affects the diameter of the fibers made at 1:2 PVA:AcZn mass ratio, when compared to the
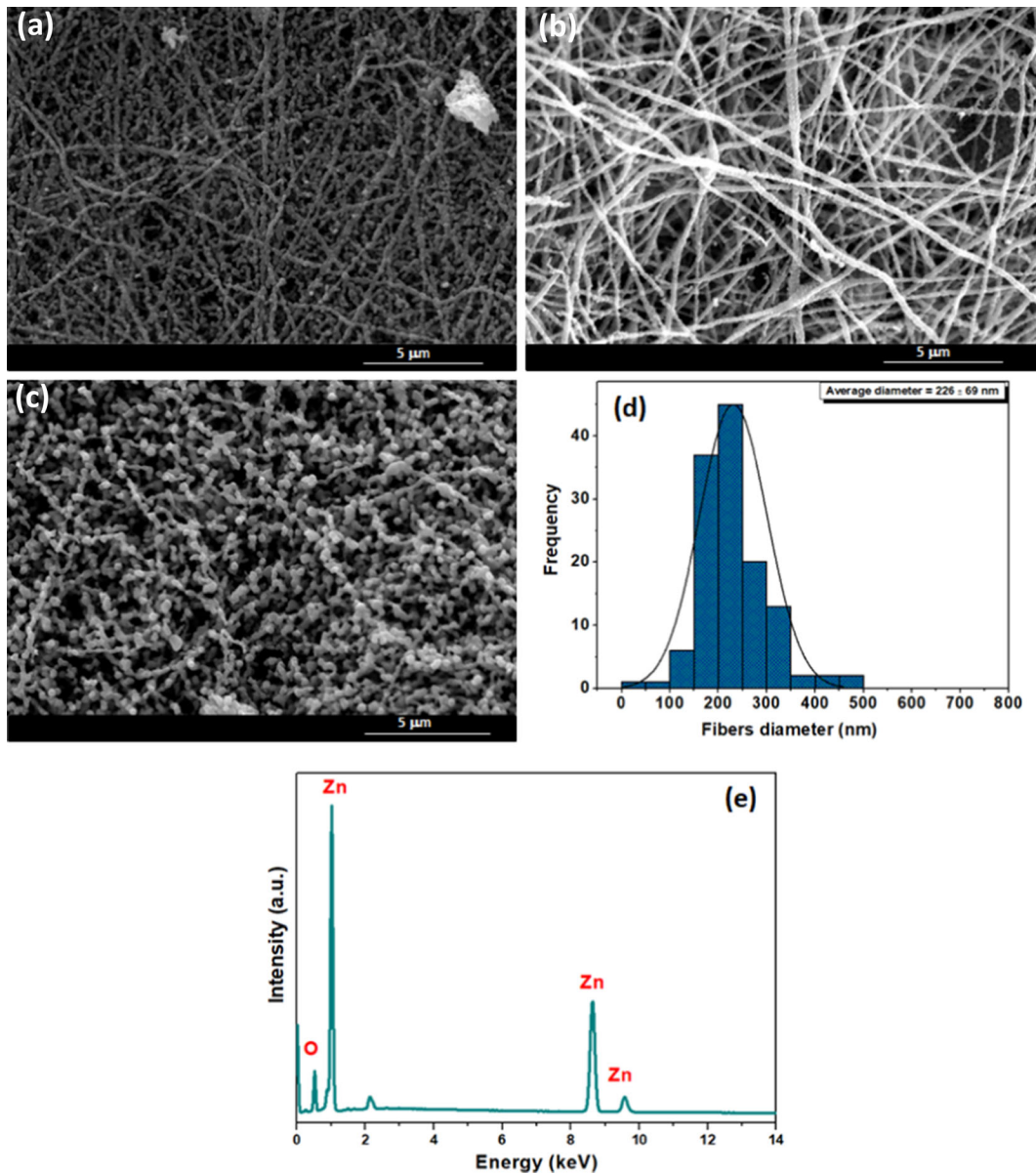
Fig. 6 SEM images of nanofibers: (a) 1:1 (500 °C), (b) 1:1 (600 °C), and (c) 1:1 (700 °C). (d) Diameter distribution histogram of 1:1 (600 °C) fibers. (e) EDS spectrum of 1:1 (500 °C) nanofibers

respective fibers 1:2 (average diameter 292 nm). According to the results presented above, it can be understood that a combination of PVA:AcZn mass ratio in the precursor fiber and annealing temperature is essential for the ZnO crystals to grow without losing the connectivity, the fiber shape, and without the presence of residues of the polymer in the final material. The results indicate that the mass ratio 1:1 and the temperature of 600 °C are, amid the studied conditions, the best since

that at this combination homogeneous ZnO fibers are obtained with morphology similar to those of the precursor fibers, but without the presence of organic matter.

The EDS spectra of samples 1:0.5 (500 °C), 1:1 (500 °C), and 1:2 (500 °C) are shown in Figs. 5(d), 6(d), and 7(d), respectively. The analysis of the elements at the surface of the samples showed the presence of Zn and O atoms. In addition, there are no other signs except what appears in the region of 2.1–2.2 eV attributed to
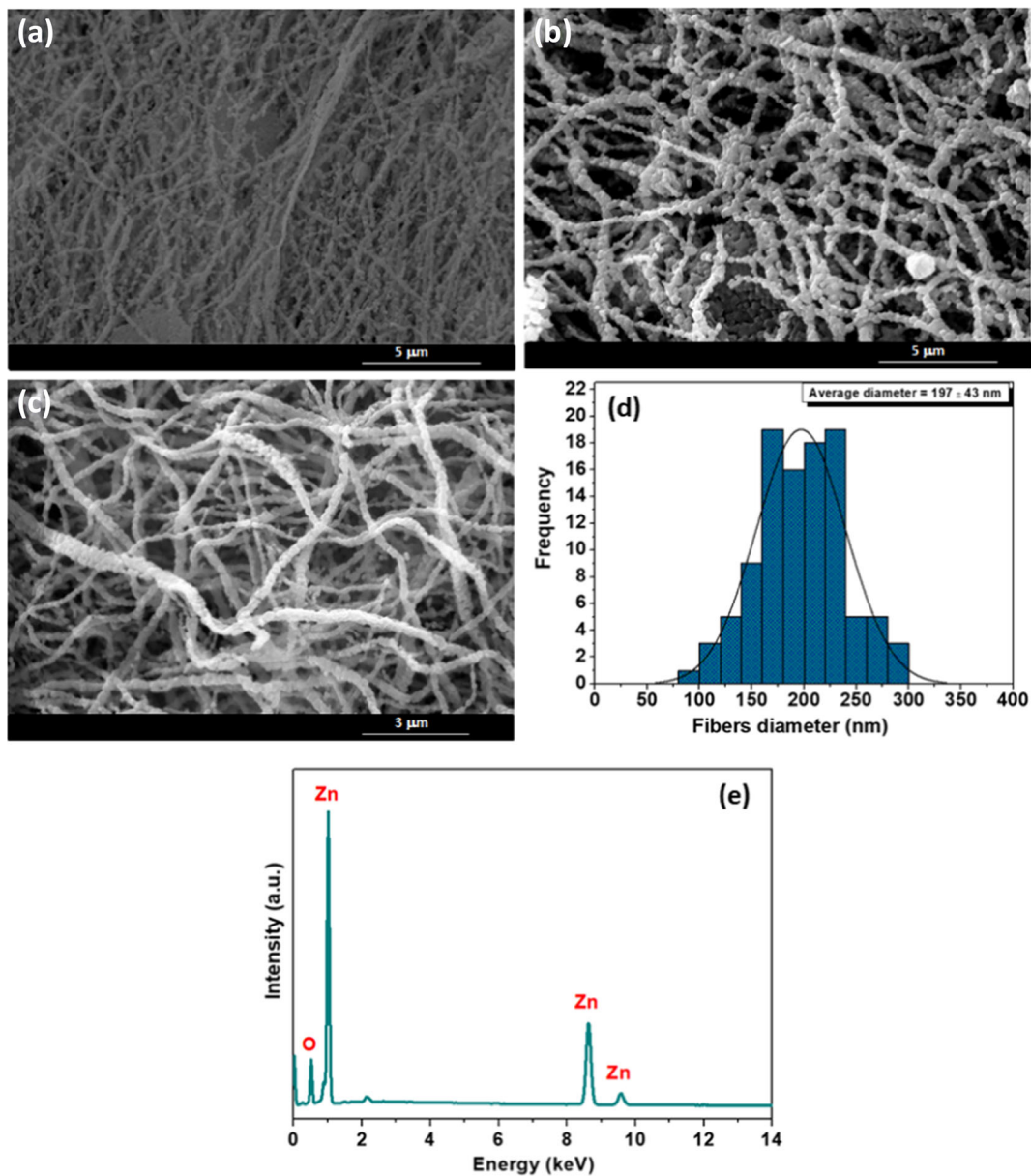
Fig. 7 SEM images of nanofibers: (a) 1:2 (500 °C), (b) 1:2 (600 °C), and (c) 1:2 (700 °C). (d) Diameter distribution histogram of 1:2 (600 °C) fibers. (e) EDS spectrum of 1:2 (500 °C) nanofibers

the element Au that covers the samples. This indicates that the removal of PVA on the fiber surface has been, probably, completed.

The distribution of Zn, C, and O atoms before and after the annealing at 600 °C of electrospun PVA:AcZn 1:1 fibers was done and the maps are presented in Fig. 8. It can be visualized that the Zn atoms are homogeneously distributed in PVA:AcZn 1:1 fibers (Fig. 8a) as well as in annealed ones (ZnO fibers, Fig. 8b), despite in ZnO

fibers, the Zn atoms are more closely together, as expected. It means that the Zn atoms are distributed in whole fibers. i.e., no diffusion in or out from fibers occurred due to the annealing process. Homogeneous distribution of C and O atoms was also observed in fibers before and after annealing (Figs. 8c–f, respectively). So, the annealing process does not affect the Zn, O, and C atom distribution. The conductivities (in 10^3 S/m) of fibers are 1.48 ± 0.037, for PVA:AcZn 1:1 and 5.68
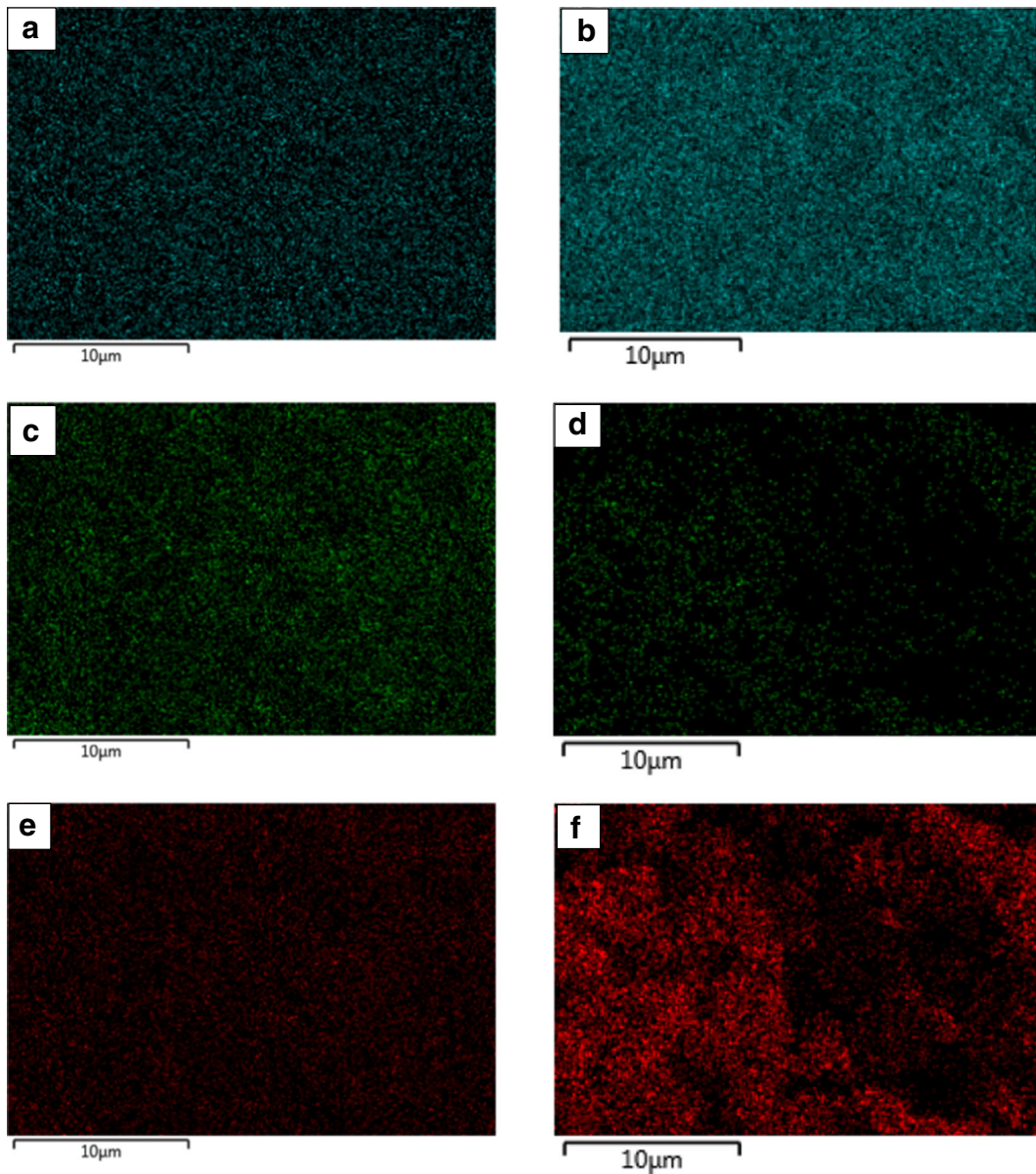
Fig. 8 EDS maps for PVA:AcZn 1:1 (left side: a, c, and e) and for the respective ZnO fibers (right side: b, d, and f) obtained through annealing at 600 °C. Map for Zn atoms (top), for C atoms (middle), and for O atoms (bottom)

± 0.07 for ZnO (obtained through annealing at 600 °C). For the sake of comparison, the conductivity (in 10^3 S/m) of ZnO powder was 7.27 ± 0.07. It means that that the coalescence of fibers due to annealing process for obtaining the ZnO fibers increased the conductivity of fibers in almost 4-folds. But the conductivity of ZnO fibers is lesser that the ZnO powder. These results match to the EDS maps for Zn on ZnO fibers as compared to PVA:AcZn fibers.

Thermogravimetric analyses were performed on ZnO fibers calcined at 500, 600, and 700 °C to evaluate if residue of organic matter is absent (or not) in these fibers. TG curves of ZnO calcined at 500 °C are shown in Fig. 9a. As shown in the thermograms, all composite nanofibers annealed at 500 °C showed traces of organic material (residual PVA or polymer decomposition products), being more evident in the composite nanofibers obtained from the solution with the lowest Zn content
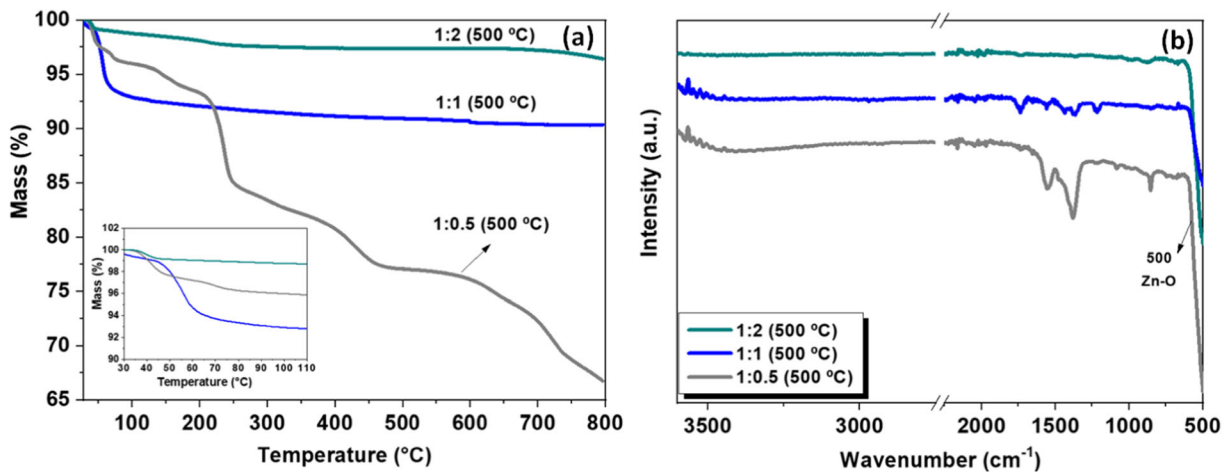
Fig. 9 (a) TG curves of the fibers: 1:0.5 (500 °C), 1:1 (500 °C), and 1:2 (500 °C); (b) FTIR spectra of the fibers: 1:0.5 (500 °C), 1:1 (500 °C), and 1:2 (500 °C)

(ratio 1:0.5) and no evidence of residues of organic material in the fibers calcined at 700 °C. In the TG curves of the nanofibers 1:1 (600 °C), 1:1 (700 °C), 1:2 (600 °C), and 1:2 (700 °C) (not shown), there is no trace or decomposition residue of PVA. Comparing this result with the EDS spectra of these same fibers, it can be inferred that the organic residue that appears in the TG curves is located mostly inside the fibers, probably more difficult to be removed from the fibers by annealing at 500 °C.

FTIR spectra of 1:0.5 (500 °C) and 1:1 (500 °C) nanofibers (Fig. 9b) showed characteristic bands of residual organic matter. These results confirm that the temperature of 500 °C was not sufficient to eliminate all organic matter and, therefore, to obtain pure ZnO nanofibers. On the other hand, annealing the fibers with PVA:AcZn mass ratio 1:2 at 500 °C produced ZnO with no evidence of organic matter. This indicates that higher

concentration of zinc aids the degradation of PVA, even at 500 °C. Thus, it is inferred that the PVA decomposition reaction must involve the formation of unstable species that is accelerated in presence of higher amount of zinc. Thus, the mass ratio PVA:AcZn 1:2 in the precursor fiber contributed to complete degradation of the polymer, even at 500 °C. These results match to the ones presented in Fig. 4. A wide band was observed in the region between 500 and 600 cm^{-1} in the FTIR spectra of the ZnO nanofibers obtained by annealing at 500 °C (Fig. 9b). Such band was attributed to vibration due to the Zn–O flexion (Velázquez-Carriles et al. 2020).

Figure 10a shows the Raman spectra of ZnO nanofibers obtained by annealing at 500 °C of PVA/AcZn nanofibers at different PV/AcZn mass ratios; the Raman spectra of 1:1 (500 °C), 1:1 (600 °C), and 1:1 (700 °C) nanofibers are shown in Fig. 10b. In all samples, active
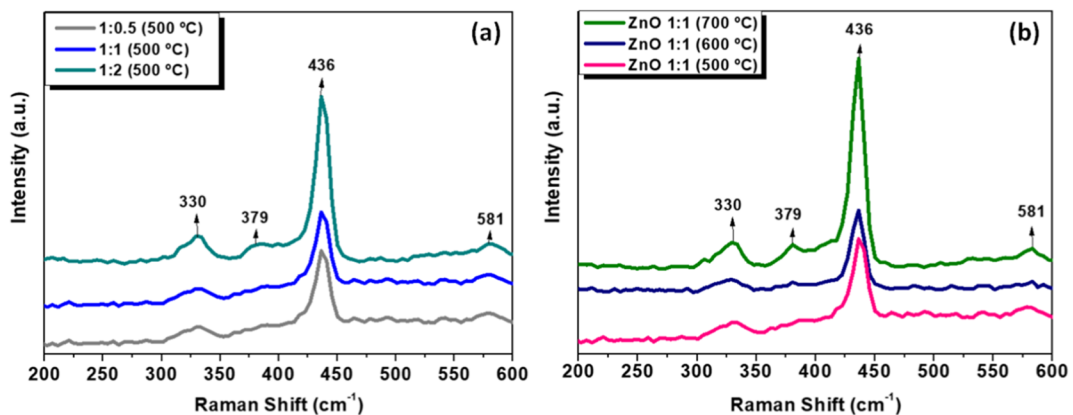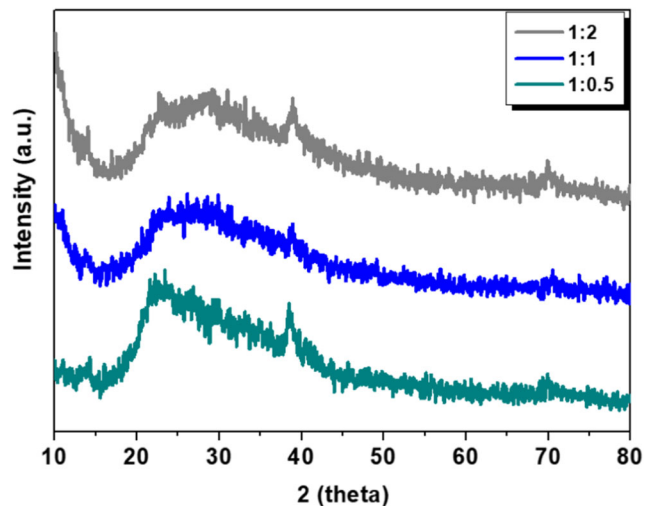

Fig. 10 Raman spectra of the fibers: (a) 1:0.5 (500 °C), 1:1 (500 °C), and 1:2 (500 °C); (b) 1:1 (500 °C), 1:1 (600 °C), and 1:1 (700 °C)

Fig. 11 WAXD diffractograms obtained from samples of precursor nanofibers at PVA/AcZn mass ratios of 1:0.5, 1:1, and 1:2

mode characteristics of ZnO were observed, for example, at 436.17 cm^{-1} (E$_2$), at 330.38 cm^{-1} (3E$_2$H-E$_2$L), at 379.36 cm^{-1} (A$_1$T), and at 580.86 cm^{-1} (B$_1$). The peak at 436.17 cm^{-1} of higher intensity identifies the hexagonal wurtzite structure of the ZnO nanofibers (Muchuweni et al. 2018), while the peak at 330.38 cm^{-1} is due to the multiple phonon scattering [38] and the peak at 580.86 cm^{-1} occurs owing to the structural defects such as oxygen vacancy (Muchuweni et al. 2018). As shown in the spectra, with the increase for AcZn in the precursor fiber, the peaks in the spectra of the ZnO fibers become thinner, characterizing the formation of more organized ZnO. For composite nanofibers annealed at 500 °C, 600 °C, and 700 °C, under the same mass ratio (1:1) (Fig. 10b), the spectra showed the same active modes, but with increase in intensity. These

changes are consequence of the increase of sample crystallinity and the growth of crystallites.

The wide-angle X-ray diffraction (WAXD) profiles of precursor nanofibers (Fig. 11) clearly show the predominance of amorphous nature. Only two signals are present in these WAXD profiles, a halo at approximately 22° and a signal at 38°, which are characteristics of the semi-crystalline structure of PVA (Das and Sarkar 2018). The presence of AcZn in the solution submitted to electrospinning does not lead to significant changes in the diffractograms. In fact, there is only a slight widening of the halo between 25 and 30° with an increase in the amount of AcZn.

The annealing of the PVA/AcZn nanofibers leads to highly crystalline structures, as shown in WAXD profiles of Fig. 12. The WAXD profile obtained from the
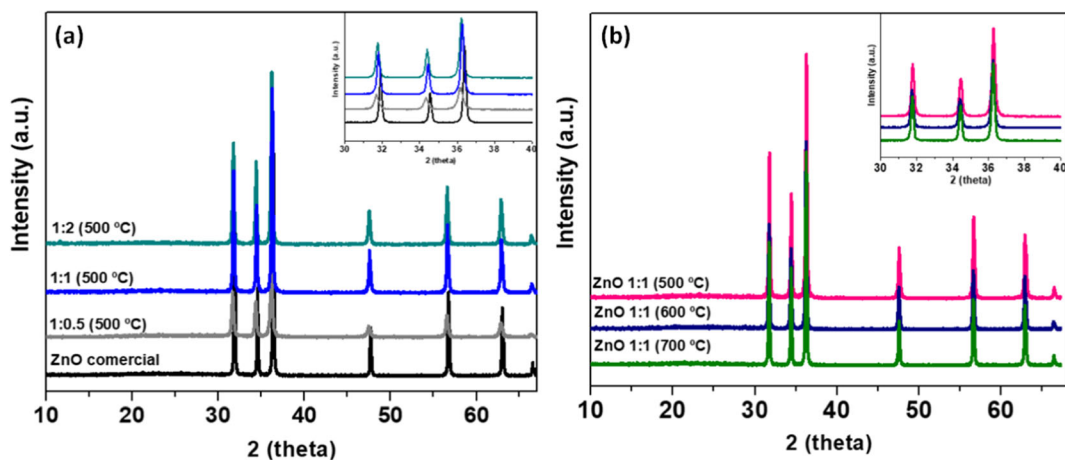

Fig. 12 XRD patterns of ZnO nanofibers: (a) 1:0.5 (500 °C), 1:1 (500 °C), and 1:2 (500 °C); and (b) 1:1 (500 °C), 1:1 (600 °C), and 1:1 (700 °C)

commercial sample of nanoparticulate ZnO was inserted in this figure, for the sake of comparison. All diffraction peaks of ZnO nanofibers annealed at different temperatures were assigned to a single-face hexagonal phase of ZnO (JCPDS card no. 36-1451), the wurtzite, with diffraction peaks at 31.8° (100), 34.4° (002), 36.2° (101), 47.5° (102), 56.5° (110), 62.9° (103), and 66.3° (200). It was observed that the increase in the amount of AcZn in precursor fibers results in more intense and thinner peaks, indicating a greater crystallinity of the pure ZnO nanofibers, as shown in Fig. 12a. In relation to the commercial ZnO, a slight shift in the diffraction signals was observed to lower values of 2θ, as shown in the WAXD profile inset in Fig. 12. The slight displacement of peaks may be related to changes in lattice parameters, such as lattice constants, unit cell volume, and grain size (Bodke et al. 2018) due to the synthesis and calcination of the material. When assessing the effect of the annealing temperature on the ZnO nanofibers (Fig. 12b), there is also a slight shift in the diffraction peaks to lower 2θ values. Thus, the displacement can be related to changes in lattice parameters with the increase in the annealing temperature. However, this variation is very small, with the influence of temperature being more reflected in the size of the crystallites.

The size of the crystallite was calculated from the (101) diffraction peak width using Scherrer's equation:

$$D = \frac{K.\lambda}{\beta.\cos\theta} \qquad (2)$$

where D is the size of the crystallite in a particular orientation, and K is a dimensionless factor, with a value close to the unit. The form factor has a typical value of about 0.9, but varies with the actual shape of the crystallite; λ is the incident X-ray wavelength, θ is the diffraction angle, corresponding to a particular orientation, and β is the width at half height (FWHM = full width at half maximum) of the diffraction peak. The obtained D values are shown in Table 2.

The analysis of data from Table 2 showed that there was a decrease in the size of the crystallite in relation to the commercial sample, and that the increase in the concentration of AcZn in the precursor fibers and in the annealing temperature lead to a slight increase in the size of the crystallite. These results show that a greater amount of AcZn results in better quality of the crystal and that the increase in the size of the crystallite with the annealing temperature is attributed to the collapse of the small crystals that, due to the sintering effect, allowing to form larger agglomerates.

The increase in the number of works published in the electrospinning area is already large but the expectation is to increase much more due to the improvements that already exist before and to the new methodologies developed in the last 15–20 years for obtaining fibrous inorganic materials, mainly of metallic oxides (Wu et al. 2013). The present work deals and discusses the methodology for obtaining ZnO nanofibers from electrospinning of poly (vinyl alcohol) solution containing zinc acetate (AcZn) and varying the PVA:AcZn mass ratio (1:0.5, 1:1, and 1:2) and the annealing temperature (500, 600, and 700 °C). Seeking for a lower temperature, for reasons of energy-cost reduction, it was found that the ZnO fibers with better characteristics (homogeneity in morphology, smaller mean diameter, organization of the crystalline lattice, among others) were obtained using mass ratio of PVA:AcZn 1:1 at temperature of 600 °C. The conductivity (ca. 80% of the conductivity of ZnO powders) of the ZnO fibers obtained from PVA:AcZn 1:1 at temperature of 600 °C and the very good crystalline organization of ZnO indicate that such materials may have interesting applications in situation where the conductive and/or

Table 2 Average diameter of the crystallite in several crystalline planes of ZnO nanofibers obtained from solutions with different PVA/AcZn mass ratios and obtained at different temperatures. Values were calculated using the Debye-Scherrer equation [29]

Samples	Annealing temperature (°C)	Average diameter size (nm)
Commercial ZnO	-	49.9
1:0.5	500	25.2
1:1	500	39.7
1:2	500	40.9
1:1	600	40.8
1:1	700	42.7

structural organization are important properties, such as solar cells and catalyst.

Conclusions

In this work, zinc oxide (ZnO) nanofibers were obtained from electrospun PVA/AcZn nanofibers. The following mass ratios PVA/AcZn 1:0.5, 1:1, and 1:2 were evaluated in the solution submitted to the electrospinning process. The PVA/AcZn fibers showed similar morphology to the PVA nanofibers; however, there was a decrease in the average diameter of the PVA/AcZn composite fibers with the increase in the amount of salt in the electrospun solution. This was attributed to electrical charges due to the presence of salt in the polymeric solution, which generates stronger repulsion between the fibers in the electrospinning process, which leads to the production of finer fibers. The ZnO nanofibers were obtained by annealing at 500, 600, and 700 °C of the precursors PVA/AcZn electrospun fibers. The annealing temperature has a strong influence on the morphology of the ZnO fibers, which have much smaller average diameters than the respective precursor fibers. In addition, organic residues in the ZnO fibers obtained by annealing the precursor fibers at 500 °C for 2 h in atmospheric air still remained. The results of TG, FTIR, and EDS indicate that the organic residues must be located inside the fiber, where it is more difficult to be removed. However, there was no evidence of organic residue in the ZnO fibers 1:2 annealed at 500 °C or those annealed at 600 or 700 °C regardless of the mass ratio PVA/AcZn. However, the 1:2 (600 °C) fibers and those obtained by annealing at 700 °C do not present the morphology of continuous fibers, but an appearance of ZnO particles connected to each other, similar to a "pearl necklace." The present work and a previous work of our research group (Oliveira et al. 2020) showed that the ZnO fibers with the best characteristics (homogeneity in morphology, smaller average diameter, organization of the crystalline lattice, among others) were obtained using mass ratio of PVA:AcZn 1:1 and calcination at 600 °C. These fibers obtained by electrospinning technique can be used for different applications, in which conductive and/or structural organization is an important property. We believe that our work can be used as a

direction for the synthesis of other highly potential materials based on metal oxide fibers.

Compliance with ethical standards

Conflict of interest The authors declare that they have no competing interest.

References

Alexandre N, Ribeiro J, Gärtner A, Pereira T, Amorim I, Fragoso J, Lopes A, Fernandes J, Costa E, Santos-Silva A, Rodrigues M, Santos JD, Maurício AC, Luís AL (2014) Biocompatibility and hemocompatibility of polyvinyl alcohol hydrogel used for vascular grafting—in vitro and in vivo studies. J Biomed Mater Res A 102(12):4262–4275. https://doi.org/10.1002/jbm.a.35098

Blachowicz T, Ehrmann A (2020) Recent developments in electrospun ZnO nanofibers: a short review. Journal of Engineered Fibers and Fabrics 15:1558925019899682. https://doi.org/10.1177/1558925019899682

Bodke MR, Purushotham Y, Dole BN (2018) Comparative study on zinc oxide nanocrystals synthesized by two precipitation methods. Cerâmica 64:91–96. https://doi.org/10.1590/0366-69132018643692207

Budrugeac P (2008) Kinetics of the complex process of thermo-oxidative degradation of poly (vinyl alcohol). J Therm Anal Calorim 92(1):291–296. https://doi.org/10.1007/s10973-007-8770-8

Cavaliere S (2016) Electrospinning for advanced energy and environmental applications. Available via http://worldcat.org. Accessed 30 Aug 2017

Chamakh M, Ayesh AI, Gharaibeh MF (2020) Fabrication and characterization of flexible ruthenium oxide-loaded polyaniline/poly (vinyl alcohol) nanofibers. J Appl Polym Sci 137(38):49125. https://doi.org/10.1002/app.49125

Costa ACS, Alves HPA, Correa MA, Bohn F, Acchar W (2019) Iron oxide/PVA flexible magnetic tape engineered by microwave combustion and tape casting. Mater Chem Phys 232:1–5. https://doi.org/10.1016/j.matchemphys.2019.04.027

Das M, Sarkar D (2018) Development of room temperature ethanol sensor from polypyrrole (PPy) embedded in polyvinyl

alcohol (PVA) matrix. Polym Bull 75(7):3109–3125. https://doi.org/10.1007/s00289-017-2192-y

Ghafari E, Feng Y, Liu Y, Ferguson I, Lu N (2017) Investigating process-structure relations of ZnO nanofiber via electrospinning method. Compos Part B 116:40–45. https://doi.org/10.1016/j.compositesb.2017.02.026

Ghafari E, Nantung T, Lu N (2019) An efficient Polyvinylidene fluoride (PVDF) nanogenerator for energy harvesting in low frequency range. ES Materials & Manufacturing 5:72–77. https://doi.org/10.30919/esmm5f321

Greiner A, Wendorff JH (2007) Electrospinning: a fascinating method for the preparation of ultrathin fibers. Angew Chem Int Ed 46(30):5670–5703. https://doi.org/10.1002/anie.200604646

Han G, Su Y, Feng Y, Lu N (2019) Approaches for increasing the β-phase concentration of electrospun polyvinylidene fluoride (PVDF) nanofibers. ES Materials & Manufacturing 6:75–80. https://doi.org/10.30919/esmm5f612

Kantürk Figen A, Coşkuner Filiz B (2019) Polymeric and metal oxide structured nanofibrous composites fabricated by electrospinning as highly efficient hydrogen evolution catalyst. J Colloid Interface Sci 533:82–94. https://doi.org/10.1016/j.jcis.2018.08.046

Kim J-H, Mirzaei A, Woo Kim H, Kim SS (2019) Combination of Pd loading and electron beam irradiation for superior hydrogen sensing of electrospun ZnO nanofibers. Sensors Actuators B Chem 284:628–637. https://doi.org/10.1016/j.snb.2018.12.120

La Porta FAT, Carlton A (2020) Emerging research in science and engineering based on advanced experimental and computational strategies, 1st edn. Springer International Publishing. https://doi.org/10.1007/978-3-030-31403-3

Li D, Xia Y (2004) Electrospinning of nanofibers: reinventing the wheel? Adv Mater 16(14):1151–1170. https://doi.org/10.1002/adma.200400719

Merritt SR, Exner AA, Lee Z, von Recum HA (2012) Electrospinning and imaging. Adv Eng Mater 14(5):B266–B278. https://doi.org/10.1002/adem.201180010

Muchuweni E, Sathiaraj TS, Nyakotyo H (2018) Effect of annealing on the microstructural, optical and electrical properties of ZnO nanowires by hydrothermal synthesis for transparent electrode fabrication. Mater Sci Eng B 227:68–73. https://doi.org/10.1016/j.mseb.2017.10.006

Mustapha S, Ndamitso MM, Abdulkareem AS, Tijani JO, Shuaib DT, Mohammed AK, Sumaila A (2019) Comparative study of crystallite size using Williamson-Hall and Debye-Scherrer plots for ZnO nanoparticles. Adv Nat Sci Nanosci Nanotechnol 10(4):045013. https://doi.org/10.1088/2043-6254/ab52f7

O'Donnell KL, Oporto-Velásquez GS, Comolli N (2020) Evaluation of acetaminophen release from biodegradable poly (vinyl alcohol) (PVA) and nanocellulose films using a multiphase release mechanism. Nanomaterials (Basel) 10(2):301. https://doi.org/10.3390/nano10020301

Oliveira VHB, Rechotnek F, da Silva EP, Marques VS, Rubira AF, Silva R, Lourenço SA, Muniz EC (2020) A sensitive electrochemical sensor for Pb2+ ions based on ZnO nanofibers functionalized by L-cysteine. J Mol Liq 309:113041. https://doi.org/10.1016/j.molliq.2020.113041

Peng S, Zhou M, Liu F, Zhang C, Liu X, Liu J, Zou L, Chen J (2017) Flame-retardant polyvinyl alcohol membrane with high transparency based on a reactive phosphorus-containing compound. R Soc Open Sci 4(8):170512. https://doi.org/10.1098/rsos.170512

Persano L, Camposeo A, Tekmen C, Pisignano D (2013) Industrial upscaling of electrospinning and applications of polymer nanofibers: a review. Macromol Mater Eng 298(5):504–520. https://doi.org/10.1002/mame.201200290

Saveh-Shemshaki N, Bagherzadeh R, Latifi M (2019) Electrospun metal oxide nanofibrous mat as a transparent conductive layer. Org Electron 70:131–139. https://doi.org/10.1016/j.orgel.2019.03.034

Sawicka KM, Gouma P (2006) Electrospun composite nanofibers for functional applications. J Nanopart Res 8(6):769–781. https://doi.org/10.1007/s11051-005-9026-9

Shingange K, Swart HC, Mhlongo GH (2019) H2S detection capabilities with fibrous-like La-doped ZnO nanostructures: a comparative study on the combined effects of La-doping and post-annealing. J Alloys Compd 797:284–301. https://doi.org/10.1016/j.jallcom.2019.05.060

Son WK, Youk JH, Lee TS, Park WH (2004) The effects of solution properties and polyelectrolyte on electrospinning of ultrafine poly (ethylene oxide) fibers. Polymer 45(9):2959–2966. https://doi.org/10.1016/j.polymer.2004.03.006

Thenmozhi S, Dharmaraj N, Kadirvelu K, Kim HY (2017) Electrospun nanofibers: new generation materials for advanced applications. Mater Sci Eng B 217:36–48. https://doi.org/10.1016/j.mseb.2017.01.001

Thomas PS, Guerbois JP, Russell GF, Briscoe BJ (2001) FTIR study of the thermal degradation of poly (vinyl alcohol). J Therm Anal Calorim 64(2):501–508. https://doi.org/10.1023/A:1011578514047

Tian H, Yuan L, Zhou D, Niu J, Cong H, Xiang A (2018) Improved mechanical properties of poly (vinyl alcohol) films with glycerol plasticizer by uniaxial drawing. Polym Adv Technol 29(10):2612–2618. https://doi.org/10.1002/pat.4374

Velázquez-Carriles CA, Carbajal-Arizaga GG, Silva-Jara JM, Reyes-Becerril MC, Aguilar-Uscanga BR, Macías-Rodríguez ME (2020) Chemical and biological protection of food grade nisin through their partial intercalation in laminar hydroxide salts. J Food Sci Technol 57:3252–3258. https://doi.org/10.1007/s13197-020-04356-y

Wang L, Haugen NO, Wu Z, Shu X, Jia Y, Ma J, Yu S, Li H, Chai Q (2019) Ferroelectric BaTiO3@ZnO heterostructure nanofibers with enhanced pyroelectrically-driven-catalysis. Ceram Int 45(1):90–95. https://doi.org/10.1016/j.ceramint.2018.09.137

Wang S, Ju J, Wu S, Lin M, Sui K, Xia Y, Tan Y (2020) Electrospinning of biocompatible alginate-based nanofiber membranes via tailoring chain flexibility. Carbohydr Polym 230:115665. https://doi.org/10.1016/j.carbpol.2019.115665

Wu H, Kong D, Ruan Z, Hsu P-C, Wang S, Yu Z, Carney TJ, Hu L, Fan S, Cui Y (2013) A transparent electrode based on a metal nanotrough network. Nat Nanotechnol 8(6):421–425. https://doi.org/10.1038/nnano.2013.84

Xie L, Jiang M, Dong X, Bai X, Tong J, Zhou J (2012) Controlled mechanical and swelling properties of poly (vinyl alcohol)/sodium alginate blend hydrogels prepared by freeze–thaw followed by Ca2+ crosslinking. J Appl Polym Sci 124(1):823–831. https://doi.org/10.1002/app.35083

Xue J, Wu T, Dai Y, Xia Y (2019) Electrospinning and electrospun nanofibers: methods, materials, and applications. Chem Rev 119(8):5298–5415. https://doi.org/10.1021/acs.chemrev.8b00593

Yang X, Shao C, Guan H, Li X, Gong J (2004) Preparation and characterization of ZnO nanofibers by using electrospun PVA/zinc acetate composite fiber as precursor. Inorg Chem Commun 7(2):176–178. https://doi.org/10.1016/j.inoche.2003.10.035

Zhang Y, Zhu F, Zhang J, Xia L (2008) Converting layered zinc acetate nanobelts to one-dimensional structured ZnO nanoparticle aggregates and their photocatalytic activity. Nanoscale Res Lett 3(6):201–204. https://doi.org/10.1007/s11671-008-9136-2

Zhang J, Lu H, Lu H, Li G, Gao J, Yang Z, Tian Y, Zhang M, Wang C, He Z (2019) Porous bimetallic Mo-W oxide nanofibers fabricated by electrospinning with enhanced acetone sensing performances. J Alloys Compd 779:531–542. https://doi.org/10.1016/j.jallcom.2018.11.269

Zhang T, Gu J, Liu X, Wei D, Zhou H, Xiao H, Zhang Z, Yu H, Chen S (2020) Bactericidal and antifouling electrospun PVA nanofibers modified with a quaternary ammonium salt and zwitterionic sulfopropylbetaine. Mater Sci Eng C 111: 110855. https://doi.org/10.1016/j.msec.2020.110855

Zhao S, Shen Y, Yan X, Zhou P, Yin Y, Lu R, Han C, Cui B, Wei D (2019) Complex-surfactant-assisted hydrothermal synthesis of one-dimensional ZnO nanorods for high-performance ethanol gas sensor. Sensors Actuators B Chem 286:501–511. https://doi.org/10.1016/j.snb.2019.01.127